Journal of Applied Polymer Science

Microencapsulated ammonium polyphosphate with boron-modified phenolic resin

Weiying Gao,[1,2,3] Shujun Wang,[1,2] Fanbin Meng,[1,2] Yuanhao Wang,[4] Huanqing Ma[1,2]

[1]State Key Laboratory of Heavy Oil Processing, China University of Petroleum, Beijing 102249, China
[2]College of Science, China University of Petroleum, Beijing 102249, China
[3]Department of Science and Technology, Chinese People's Armed Police Force Academy, Langfang 065000, China
[4]Faculty of Science and Technology, Technological and Higher Education Institute of Hong Kong, New Territories, Hong Kong
Correspondence to: S. Wang (E-mail: 598736164@qq.com or bjwsjbi@sina.com)

ABSTRACT: Ammonium polyphosphate (APP) was encapsulated with boron-modified phenolic resin (BPF) by *in situ* polymerization with the goal of improving its hydrophobicity, thermal stability, and compatibility in polymers. The chemical and physical features of APP microcapsules were characterized by Fourier transform infrared, X-ray photoelectron spectroscopy, scanning electron microscopy, inductively coupled plasma, and laser particle sizing. The hydrophobicity was assessed by the water contact angle. The residues from thermogravimetric analyzer and muffle burner were investigated. The results showed that the APP microcapsules with BPF shell had been achieved successfully. The shell encapsulation rate mainly depended on the amount of crosslinking agent when the ratio of APP/BPF was constant. The mean particle size increased and the particle size distribution became more narrow. The hydrophobicity of APP was improved and the improvement degree mainly depended on the amount and adding rate of crosslinking agent and the conditions of heat curing. A good thermal stability and high residue char rate at high temperature were noticed for APP microcapsules. It suggests that these microcapsules might be used as an intrinsic flame retardant. © 2016 Wiley Periodicals, Inc. J. Appl. Polym. Sci. **2016**, *133*, 43720.

KEYWORDS: coatings; properties and characterization; surfaces and interfaces; thermal properties

Received 25 December 2015; accepted 31 March 2016
DOI: 10.1002/app.43720

INTRODUCTION

Because of its low smoke, low toxicity, and the lack of corrosive substances produced during its combustion, ammonium polyphosphate (APP) $[(NH_4)_{n+2}P_nO_{3n+1}]$ is widely used as flame retardant in coatings industry, plastics, wood, rubber or as extinguisher in forest fires, coal field fires. When exposed to an external heat flux, APP would play a role as acid source to react with carbon source and gas source to give off inert gas, for example N_2, NH_3, CO_2, and form an intumescent carbonaceous char layer as a kind of physical barrier to inhibit the transfer of heat and diffusion of inflammable gases.[1–4] Unfortunately, The fire retardancy of APP is not permanent due to its weak water resistance and poor compatibility in polymers. Microencapsulation technique is a good choice to overcome above problems. Microencapsulation is a technique, with which solid or liquid could be encapsulated by a film-forming material to form tiny particles. The encapsulated solid or liquid core is isolated from the environment, thus the property of the core is reserved completely. Under appropriate condition, the core material can be released for action when the shell is being destroyed. In previous study by Wu *et al.*, microcapsules containing APP with various shells, such as melamine-formaldehyde, nylon-6, ureaformaldehyde, epoxy resin, and gel-silica, were reported.[5–11] To a certain extent the water resistance and compatibility of APP encapsulated by these shells have been improved. However, some shortcomings still exist, such as incomplete coating, complicated process flow or low residue char rate, so a study on new shell material or new method is necessary. To the best of our knowledge, microcapsules containing APP with boron-modified phenolic resin (BPF) shell has not yet been reported.

The BPF is a modified phenolic resin whose three-dimensional network structure is obtained by introducing boron into the main chain of a phenolic resin. The research on BPF have been begun by ChrysIer Corporation of the United States since 1950s.[12] Nobel Corporation began to produce goods in 1960s, named trolifan1200.[13] The solid-state preparation method and aqueous preparation method were reported to prepare BPF.[14–17] The BPF was mainly prepared from phenol, boric acid and formaldehyde in the early stage. Now different kinds of phenol, such as bisphenol-A, bisphenol-F, o-cresol, and so on, have been used to prepare better

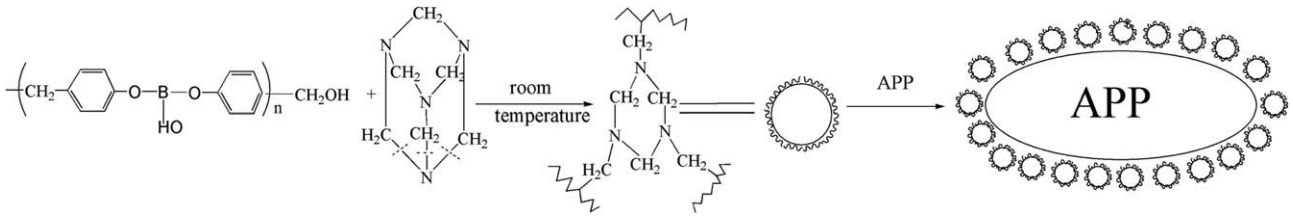

Scheme 1. Schematic diagram of reaction steps involved in the preparation of APP microcapsules.

BPF.[18,19] Because of the introduction of B—O band, the thermostability and the ablation resistance of BPF are much better than common phenolic resin and it is widely used as adhesive agent, insulation material, flame retardant material, and so on. But it has not been reported that the BPF improve the thermostability and residue rate of APP in the form of microcapsule shell so far. Besides, the mechanical properties of BPF have been improved due to the flexibility of B—O bond,[20,21] and it is hydrophobic and easily compatible with polymer. Based on above mentioned advantages, a novel type of APP microcencapsulated with BPF (BPFAPP) was prepared in this article. Emphasis was placed on the factors affecting the hydrophobicity and thermal stability of APP microcapsules.

EXPERIMENTAL

Materials

APP (core material) with an average degree of polymerization $200 < n < 400$ was supplied by Wuhan Hongxinkang Fine Chemical Corporation Limited, China. BPF (film-forming material) was purchased from Anhui Tianyu High Temperature Resin Material Corporation Limited. Alkylphenols polyoxyethylene (OP-10) and dimethylsilicon oil were supplied by Tianjin Tianli Chemical Reagent Corporation Limited, China. Hexamethylene tetramine (HMTA) was supplied by Tianjin Damao Chemical Reagent Corporation Limited, China. Ethanol and chloroform were supplied by Tianjin Fuchen Chemical Reagent Corporation Limited, China.

Preparation of Microcapsules. In the general procedure for the preparation of the microcapsules, the two solutions used are as follows:

1. Ethanol solution of BPF (50 g BPF was comminuted with a high speed disintegrator and then dissolved in 50 g ethanol);
2. Solution of HMTA (10 g HTMA was dissolved in 100 g chloroform)
3. Preparation of BPFAPP

A 250 mL three-necked round bottom flask was equipped with a mechanical stirrer. Then, 7.2 g 50% BPF solution and 64.8 g ethanol were poured into the flask and the mixture was stirred (300 rpm) for 5 min at room temperature. Then, 10 g APP, 1 g OP-10, and 0.5 g dimethylsilicon oil were added and stirred for 15 min. After that the appropriate amount of HMTA solution was added dropwise to the mixture, keeping at the same temperature for 1 h. Finally the mixture was filtered, washed with ethanol, and dried at 60 °C to achieve the final microcapsulated APP powders. The schematic route for the preparation of APP microcapsules is shown in Scheme 1. In order to further investigate the influence of heat curing on the hydrophobicity of microcapsules, some samples were cured at different temperature. The coating mechanism is as follows: The BPF was crosslinked by HTMA and then precipitated on APP from solute. The precipitated BPF particles exist as nanosize solid particles. The final microcapsulated structure is stable owing to the adsorption force between APP and BPF particles.

If a special note was not made, the following BPFAPP was prepared under the condition that the HTMA/BPF mass ratio was 0.125 and the adding rate of HTMA solution was 0.113 mL/min.

Measurements

Fourier Transforms Infrared (FTIR) Analysis. FTIR spectra were obtained on a JASCO480 spectrometer (German Bruker) with thin KBr as the sample holder. Transmission mode was used with the wave number range from 4000 to 500 cm^{-1}.

X-ray Photoelectron Spectroscopy (XPS). The XPS spectra were obtained on a K-Aepna spectrometer (Thermo Fisher Scientific) with Al Kα excitation radiation ($h\nu = 1253.6$ eV) in ultrahigh vacuum conditions.

Scanning Electron Microscopy (SEM). The morphologies of APP and BPFAPP after gold sputtering were studied using a Quam ta2000 (FEI, Czech) SEM.

Inductively Coupled Plasma (ICP). The shell encapsulation rate of APP microcapsules was calculated by the following equation:

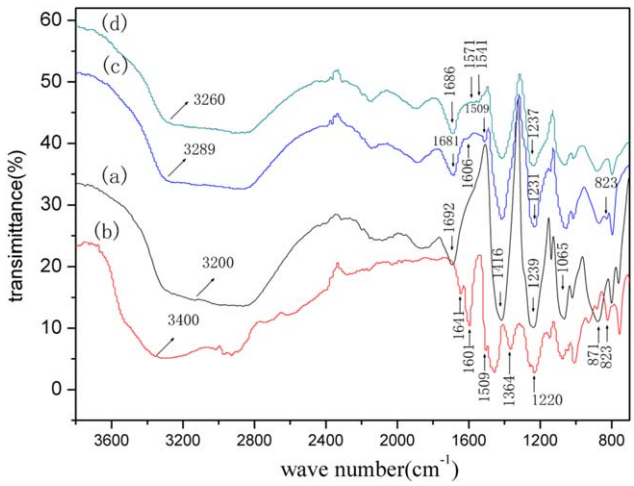

Figure 1. FTIR spectra of (a) APP, (b) BPF, (c) BPFAPP, and (d) BPFAPP-heat curing. [Color figure can be viewed in the online issue, which is available at wileyonlinelibrary.com.]

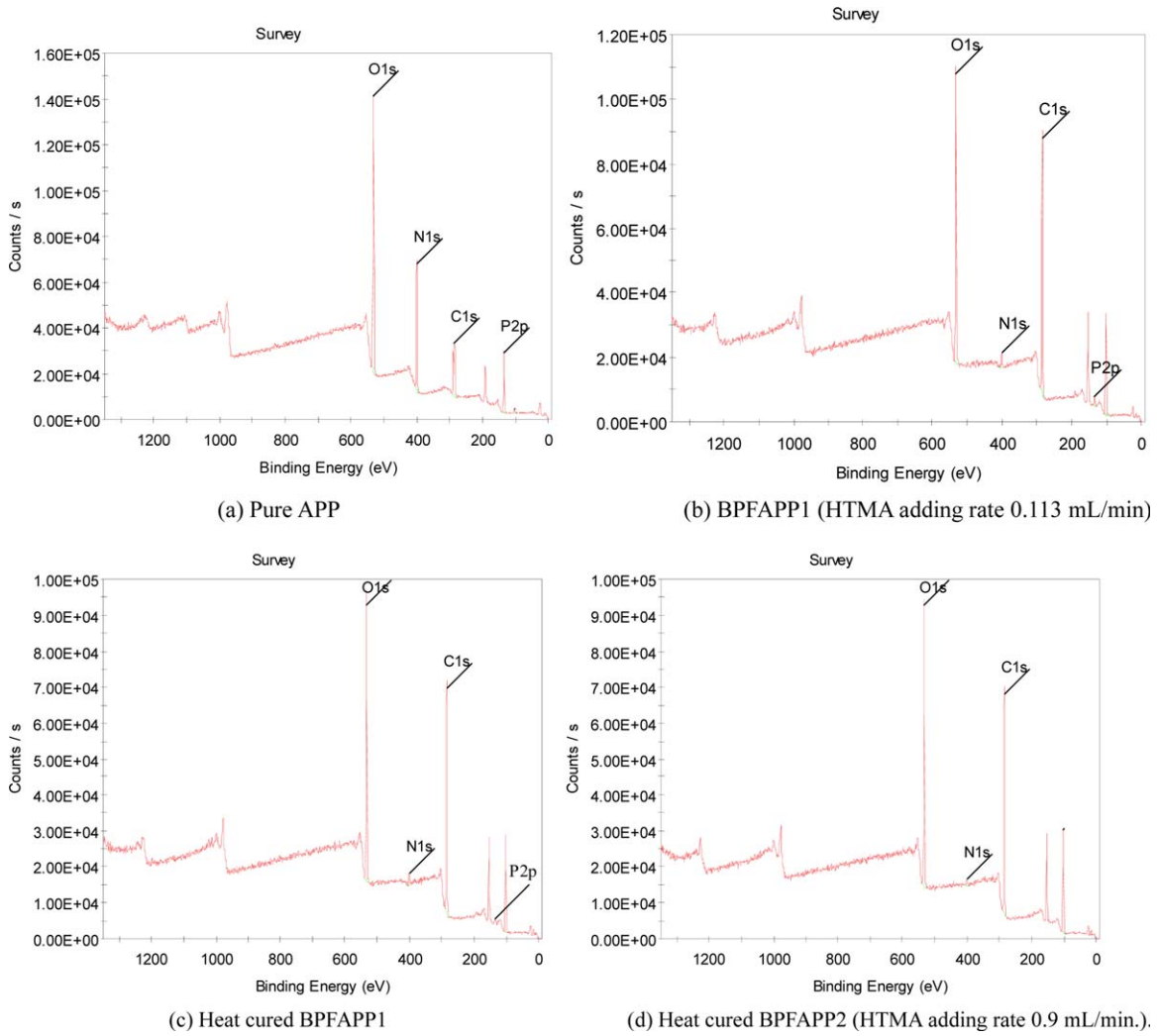

Figure 2. XPS spectra of APP and BPFAPPs. [Color figure can be viewed in the online issue, which is available at wileyonlinelibrary.com.]

$$W_{BPF}(\%) = \frac{M_2 - M_1}{M_1} = \frac{M_2}{M_1} - 1 = \frac{P_1}{P_2} - 1$$

Where M_1 and M_2 are the mass of neat APP and APP microcapsules respectively, P_1 and P_2 are the mass percent (%) of phosphorous in APP and APP microcapsules obtained by ICP. The phosphorous contents of APP and APP microcapsules, digested with the molar ratio of 3:1 mixed acid of sulphuric acid and nitric acid, were measured using an ICP atomic emission spectrometer (Thermo Fisher Scientific).

Hydrophobicity Analysis. The hydrophobicity of samples was characterized by contact angle between the powders and deionized water. The powder samples, pressed into wafers at 15 MPa, were measured using JC2000D contact angle analyzer (Shanghai Zhongchen Digital Technology Equipment Co., China).

Particle Size Distribution Measurement. The mean particle size and size distribution of APP and BPFAPP were measured by Laser particle sizing instrument (LS320) of Beckman Coulter, Inc. Before the measurement, the samples were dispersed in ethanol and sonicated and circulated for 20 min.

Thermogravimetric Analysis. Each sample was examined on a SDT Q600 thermogravimetric (TG) analyzer at a heating rate of 10 °C/min in N_2 atmosphere. All samples of about 3–10 mg were kept in an open Pt pan and heated from room temperature to 800 °C.

In order to study macroscopies of residues, each sample of about 1 g was kept in an open ceramic crucible in muffle furnace and heated at 10 °C/min from room temperature to 800 °C in air atmosphere.

RESULTS AND DISCUSSION

Chemical Characterization

The FTIR spectra of APP, BPF, BPFAPP, and BPFAPP-heat curing are presented in Figure 1. As seen in Figure 1(a), the important characteristic absorption bands of APP are as follows: 3200 cm^{-1} (N—H symmetric stretching vibration), 1692 cm^{-1} (N—H bending vibration), 1239 cm^{-1} (P═O), 1065 cm^{-1} (P—O symmetric stretching vibration), 871 cm^{-1} (P—O asymmetric stretching vibration), 1020 cm^{-1} (PO_2 and PO_3), and 800 cm^{-1} (P—O—P). After being coated by BPF, the spectra of BPFAPP showed new absorption bands which could be assigned

Table I. Surface Elemental Composition of APP and BPFAPPs

	APP		BPFAPP1		H-BPFAPP1		H-BPFAPP2	
Binding	Peak BE	Wt %	Peak BE	Wt %	Peak BE	Wt %	Peak BE	Wt %
P_{2p}	134.24	12.98	133.92	1.8	134.08	1.35	No	No
N_{1s}	400.26	25.09	400.15	3.12	400.23	2.61	399.63	1.63
O_{1s}	532.06	34.1	531.89	23.03	532.09	23.09	532.1	23.09
C_{1s}	285.04	25.72	284.16	48.51	284.43	51.17	284.41	50.4

APP, ammonium polyphosphate; BPFAPPs, boron-modified phenolic resin ammonium polyphosphate.

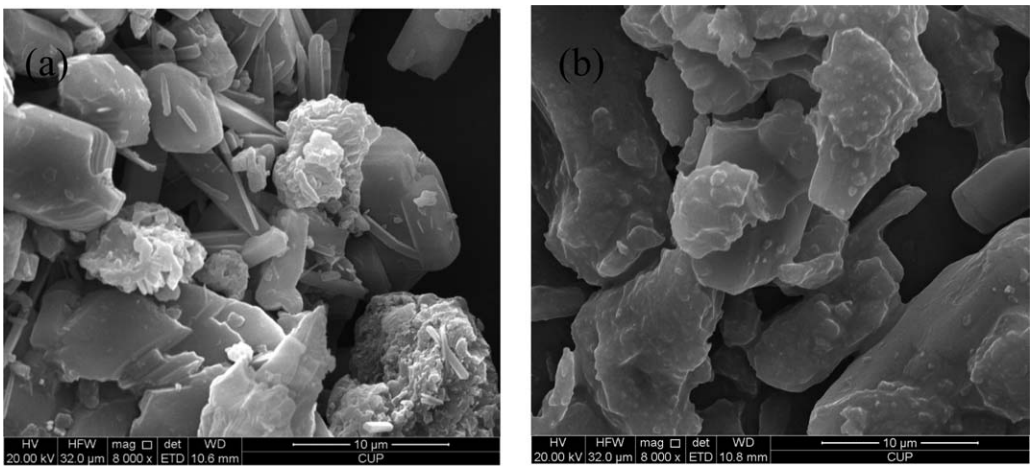

Figure 3. SEM photographs of (a) APP and (b) BPFAPP.

to BPF groups:benzene group C═C at 1606 cm^{-1} and C—C at 1509 cm^{-1}, CH_2 at 823 cm^{-1},[22] combination band of N—H (1692 cm^{-1}) and C═O (1641 cm^{-1}) at 1686 cm^{-1}, combination band of P═O (1239 cm^{-1}) and C—O (1220 cm^{-1}) at 1231 cm^{-1}, combination band of ϕ—OH or B—OH (3400 $cm^{-1)}$ and N—H (3200 cm^{-1}) at 3289 cm^{-1}, as seen in Figure 1(b,c). After being cured by heat, the absorption band of BPFAPP at 823 cm^{-1} disappeared probably as a result of the oxidation of CH_2. The reduction of hydroxyl owing to dehydration or ϕ—OH oxidized to ϕ═O leaded to the combination bands at 1686 cm^{-1} drifting down to 1681 cm^{-1},1231 cm^{-1} drifting up to 1237 cm^{-1}, 3289 cm^{-1} drifting down to 3260 cm^{-1}. Because of the conjugate effect between C═O and benzene ring, the benzene group C═C at 1606 cm^{-1} and C—C at 1509 cm^{-1} drifted to 1571 cm^{-1} and 1541 cm^{-1}, respectively.

The XPS spectra of APP and BPFAPPs are shown in Figure 2. The related surface elemental compositions of APP and BPFAPPs are recorded in Table I. It can be seen from Figure 2(a) that the peaks at 134.24, 400.26, 285.04, and 532.06 eV are assigned to P_{2p}, N_{1s}, C_{1s}, O_{1s} of APP. After microencapsulation by BPF, the intensities of P_{2p}, N_{1s}, and O_{1s} peaks greatly decreased. The P, N, O atom

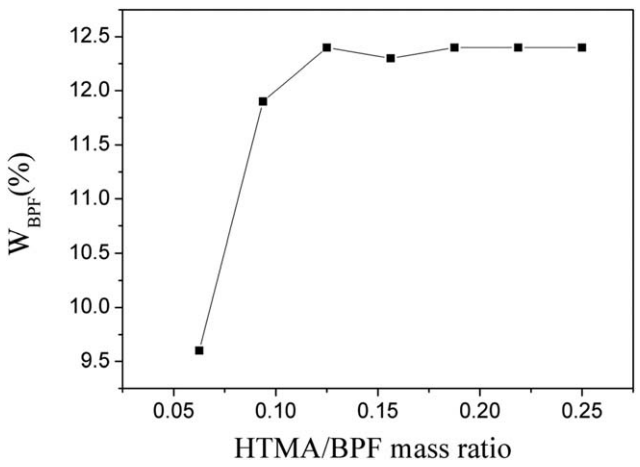

Figure 4. Influence of the HTMA amount on W_{BPF} (%).

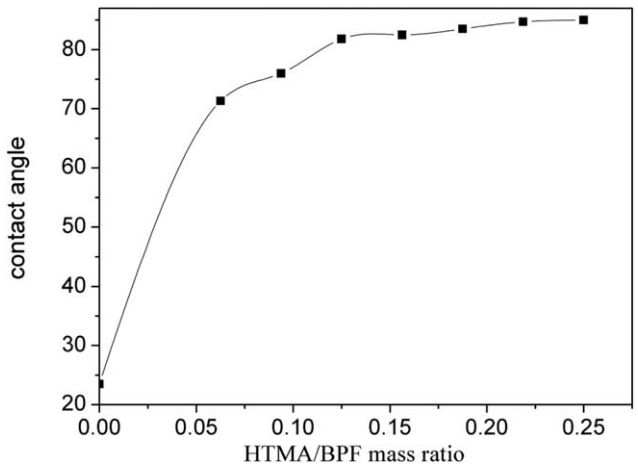

Figure 5. Influence of the amount of HTMA on BPFAPP hydrophobicity.

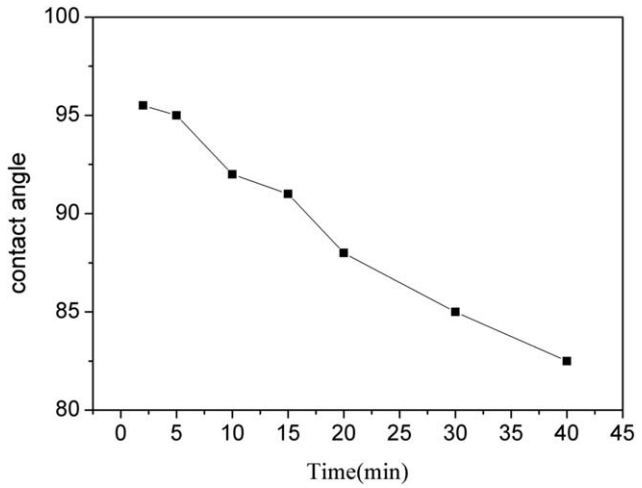

Figure 6. Influence of the HTMA adding rate on BPFAPP hydrophobicity.

content of BPFAPP1 (the HTMA solution adding rate 0.113 mL/min) was, respectively, 1.8%, 3.12%, and 23.03%, which were much lower than that of pure APP (12.98%, 25.09%, and 34.1%). Meanwhile, the intensities of the C_{1s} peaks, centered at 285.04 eV, increased sharply. The C atom content was 48.51%, higher than that of APP (25.72%), as seen in Figure 2(b) and Table I. The above changes indicate that APP is well coated by BPF.

The intensities of P_{2p} and N_{1s} peaks further decreased, yet the intensities of C_{1s}, O_{1s} increased when BPFAPP1 was cured at 160 °C for 3 h, as seen in Figure 2(c). The changes showed that APP was better coated by BPF owing to thermo-crosslinking between hydroxyls. Figure 2(d) is a spectrum of BPFAPP2 which was prepared by adding amine crosslinking agent quickly (0.9 mL/min) and cured at 160 °C for 3 h. It was found that there was no P_{2p} absorption peak and only N_{1s} peaks appeared due to the presence of amine, but the intensity was very low, which indicated that APP was completely coated by BPF. Comparisons of the above results show that heat curing and adding crosslinking agent quickly are helpful to improve the effect of microencapsulation.

Morphologies of APP and BPFAPP

The surface morphologies of APP and BPFAPP particles are shown in Figure 3. It was clear that the surface of most APP particles was very smooth. After microencapsulation, BPFAPP presented a comparably rough surface and the particles morphology and size had changed. There were a lot of little particles accumulated on the surface of APP. The above characteristics indicate that APP is well coated by BPF.

The Shell Encapsulation Rate of APP Microcapsules

Figure 4 presents the influence of the amount of amine crosslinking agent (HTMA) on the shell encapsulation rate [W_{BPF} (%)] of APP microcapsules (the HTMA solution adding rate being 0.113 mL/min). The W_{BPF} (%) varied from the HTMA amount. At first the W_{BPF} (%) sharply increased with the increase of the HTMA amount and reached maximum 12.4 when the HTMA/BPF mass ratio was 0.125. The W_{BPF} (%) appeared no more increase when the HTMA/BPF mass ratio further increased more than 0.125.

Hydrophobicity of APP and BPFAPP

The hydrophobicity of BPFAPP microcapsules is influenced by the properties of the shell material itself, encapsulation rate and coating homogeneity and so on, so the related research was performed. The water contact angle (WCA) of neat BPF crosslinked by HTMA (the HTMA/BPF ratio of 0.125) is respectively 95.5° and 108° before and after heat curing at 160 °C for 3 h.

Influence of the Amount of Crosslinking Agent Added. Figure 5 shows the influence of the amount of crosslinking agent on the hydrophobicity of BPFAPP (the HTMA solution adding rate being 0.113 mL/min). The curve was composed of three steps according to the WCA increase rate. The WCA of original APP was 23° showing that APP was very hydrophilic. After microencapsulation, the WCA sharply increased from 23°–71° at first stage due to the rapid increase of W_{BPF} (%), fast from 71° to 81° at second stage due to the formation of B—N coordinate bond and the increase of W_{BPF} (%) with the HTMA amount increasing. Although the W_{BPF} (%) increased no more at third stage, the contact angle still slowly increased from 81° to 85° due to the increase of B—N coordinate bond. However, the WCA could not always reach 95.5° even when the HTMA/BPF ratio was more than 0.125, which showed that APP had not been completely coated. The main reason is not because the precipitated BPF is not enough, but the shell is not uniform and tight.

Influence of the Adding Rate of Crosslinking Agent. Figure 6 presents the influence of the adding rate of HTMA on the hydrophobicity of BPFAPP (the HTMA/BPF mass ratio being 0.125). The WCA increased with the increase of the adding rate

Table II. The WCAs at Different Heat Curing Temperature and Time

	Temperature (°C)			ΣR	ΣR^2
Time (h)	120	160	180		
1	97.5	103	105	305.5°	31,140.25°
2	98.75	104.25	105.5	308.5°	31,749.875°
3	100.25	105	107	312.25°	32,524.0625°
ΣX	296.5	312.25	317.5	926.25°	
ΣX^2	29,307.88	32,502.06	33,604.25		95,414.19°

WCAs, water contact angles.

Table III. Analysis of Variance

Source	SS	DF	MS	*F*	$F_{.05}$
Intergroups	87.625°	2	39.8125°	424.67*	6.94
Intragroups	79.625°	2	3.8125°	40.67*	6.94
Error	0.375°	4	0.09375°		
Total	87.625°	8			

SS, sum of the squares; DF, degree of freedom; MS, mean squares; F, ratio of MS group/MS error.
* indicates that the *F* value is significant at the .05 level.

of HTMA. The WCA was more than 95° when the adding rate of HTMA was more than 0.9 mL/min. The results show that the faster HTMA is added, the more tight and uniform APP were coated owing to crosslinking quickly between HTMA and BPF, and APP could be completely coated when the adding rate of HTMA was more than 0.9 mL/min, which was also confirmed by XPS spectra (c) and (d).

Influence of the Heat Curing Temperature and Time. Table II shows the WCAs of BPFAPP (82° without heat curing) at different heat curing temperature and time. It can be seen that the WCA remarkably increased due to the removal of some hydroxyls and the formation of lipophilic groups after heat curing, which was also confirmed by XPS spectra (b) and (c). However, the WCAs varied from heat curing temperature and time. The influence degree of heat curing temperature and time on the WCAs of BPFAPP were investigated and an analysis of variance (ANOVA) was done and recorded in Table III. The intergroups F value of 424.67 assigned to temperature was larger than the $F_{.05}(2,4)$ value of 6.94, the Intragroups F value of 40.67 assigned to time was also larger than the $F_{.05}(2,4)$ value of 6.94. The results show that the temperature and time effects are very significant, but the temperature effect is more significant.

Some WCA photographs are shown in Figure 7. It was clear that the WCA of APP sharply increased after microencapsulation and further increased after heat curing.

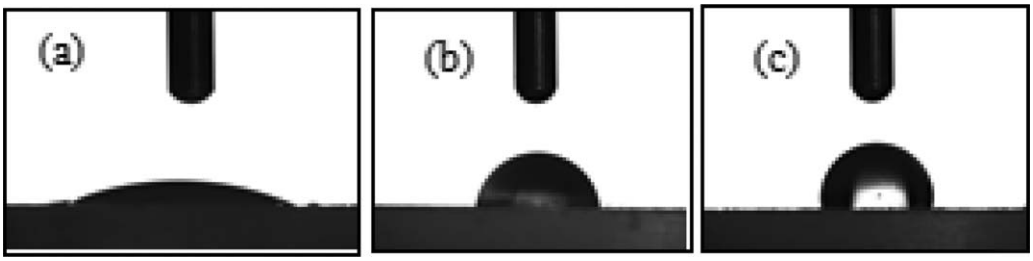

Figure 7. WCA photographs: (a) neat APP, (b) BPFAPP without heat curing, and (c) BPFAPP cured at 160 °C for 3 h.

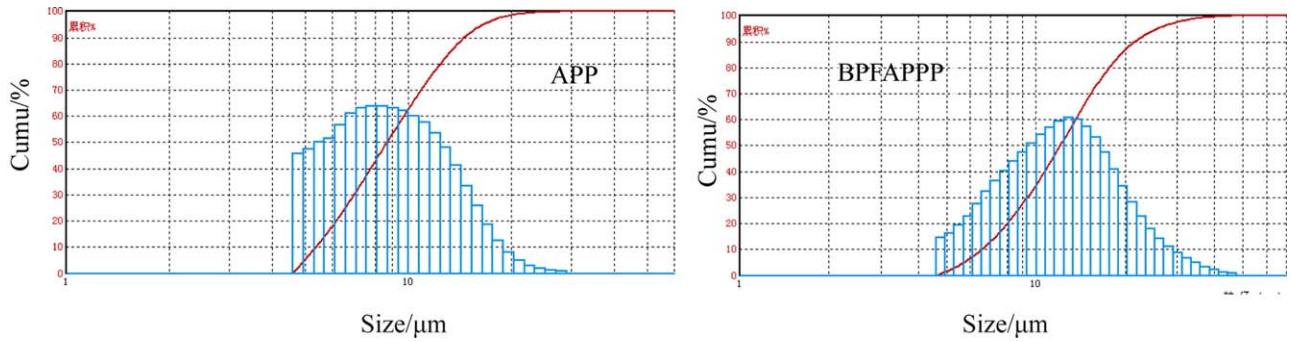

Figure 8. Size distributions of (a) APP and (b) BPFAPP. [Color figure can be viewed in the online issue, which is available at wileyonlinelibrary.com.]

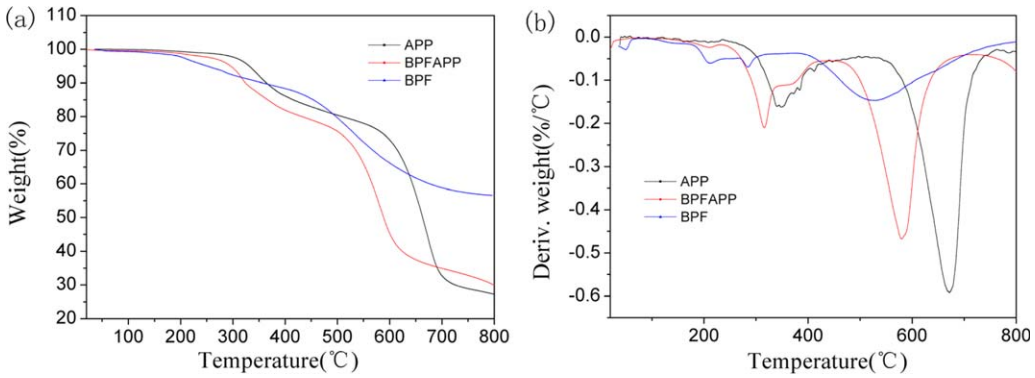

Figure 9. TG and DTG curves of APP, BPFAPP, and BPF. [Color figure can be viewed in the online issue, which is available at wileyonlinelibrary.com.]

Figure 10. Residues macroscopies of APP and BPFAPP. [Color figure can be viewed in the online issue, which is available at wileyonlinelibrary.com.]

Besides, the powder of BPFAPP turned yellow after heat curing and the color would gradually deepen with the increase of temperature and the extension of time. The BPFAPP powder cured at 160 °C for 1–3 h turned very beautiful orange but turned brown at 180 °C for 1–3 h. Comprehensively considering the hydrophobicity, color, and economical efficiency, the BPFAPP powder cured at 160 °C for 1–3 h is better.

Particle Size Distribution Measurement

The particle size distributions of APP and BPFAPP are shown in Figure 8. The mean particle size of APP increased from 9.93 to 13.32 μm and the particle size distribution of BPFAPP became more narrow than neat APP. There might be two reasons for the size change of particles. One reason is that the particles are coated by BPF, the other reason is that small particles cling to each other due to BPF viscidity.

Thermal Stability

TG and derivative thermogravimetric (DTG) curves of APP, BPFAPP, and BPF in nitrogen atmosphere are shown in Figure 9. The initial decomposition temperature (T_0) and solid residue left at 800 °C were obtained from the TG curve, as seen in Figure 9(a); The temperature of the maximum mass loss rate (T_{max}) of samples was obtained from the DTG curve, as seen in Figure 9(b).

The thermal degradation of APP was composed of two steps according to the two DTG peaks (349 and 670 °C). Its T_0 was about 304 °C. The first stage corresponded to a weight loss of 19.3%. The first stage mainly evolves in the elimination of ammonia and the formation of a highly crosslinked polyphosphoric acid (PPA). The second stage occured above 619 °C, which correspond to PPA evaporation and/or dehydration to P_4O_{10} which sublimes.[23] There was about 27.2% residue left at 800 °C. Compared with APP, the degradation of BPFAPP was similar to APP, it had two decomposition steps with the T_{max} at 315 and 580 °C, respectively, decomposing earlier than APP due to small molecular substances decomposition or dehydrating of BPF shell. However, its maximum weight loss rate in the second step was lower than that of APP. BPFFAPP was more stable than APP beyond the temperature of 690 °C. It is speculated on the formation of a char which has a better performance to resist the further degradation. Furthermore, the residue of BPFAPP at 800 °C was 30.14%, a little higher than that of APP.

APP and BPFAPP were heated in muffle furnace at 10 °C/min from room temperature to 800 °C in air atmosphere. The residues macroscopies are shown in Figure 10. It can be seen that there were little residues at the bottom of the APP crucible, but there were some residues which were mainly made of char in BPFAPP crucible.

CONCLUSIONS

In this article, APP was microencapsulated with BPF by *in situ* polymerization. FTIR, XPS, and SEM analysis showed that the APP microcapsules with BPF shell had been achieved successfully. ICP analysis showed the shell encapsulation rate [W_{BPF} (%)] mainly depended on the amount of crosslinking agent when the ratio of APP/BPF was constant. The W_{BPF} (%) increased with the HTMA/BPF mass ratio increased at first and did not increase any more when the HTMA/BPF mass ratio was more than 0.125. After microencapsulation, the hydrophobicity of APP was improved and the improvement degree mainly depended on the amount and adding rate of crosslinking agent and the conditions of heat curing. Particle size results showed that the mean particle size of APP microcapsules increased and the particle size distributions became more narrow.

From TG analysis, a good thermal stabilization and residue char at high temperature were noticed for APP microcapsules. The residue of BPFAPP at 800 °C was 30.14%, higher than that of APP (27.2%), which suggests that these microcapsules might be used as an intrinsic flame retardant. Further work is necessary on testing the fire behavior of fire retardant materials containing this type of microcapsules.

ACKNOWLEDGMENTS

The work was financially supported by the Science & Technology Program of Guangxi, China (No. 1348013-4).

REFERENCES

1. Chen, Y. H.; Liu, Y.; Wang, Q.; Yin, H.; Aelmans, N.; Kierkels, R. *Polym. Degrad. Stabil.* **2003**, *81*, 215.
2. Saihi, D.; Vroman, I.; Giraud, S.; Bourbigot, S. *React. Funct. Polym.* **2005**, *64*, 127.
3. Ni, J. X.; Chen, L. J.; Zhao, K. M.; Hu, Y.; Song, L. *Polym. Adv. Technol.* **2011**, *22*, 1824.
4. Saihi, D.; Vroman, I.; Giraud, S.; Bourbigot, S. *React. Funct. Polym.* **2006**, *66*, 1118.
5. Lin, M.; Yang, Y.; Xi, P.; Chen, S. L. *J. Appl. Polym. Sci.* **2006**, *102*, 4915.
6. Wu, K.; Zhang, Y. K.; Hu, W. G.; Lian, J. T.; Hu, Y. *Comp. Sci. Technol.* **2013**, *81*, 17.
7. Liu, M. F.; Liu, Y.; Wang, Q. *Macromol. Mater. Eng.* **2007**, *292*, 206.
8. Wu, K.; Song, L.; Wang, Z. Z.; Hu, Y. *J. Polym. Res.* **2009**, *16*, 283.

9. Wu, K.; Song, L.; Wang, Z. Z.; Hu, Y. *Polym. Adv. Technol.* **2008**, *19*, 1914.
10. Giraud, S.; Salaüna, F.; Bedek, G.; Vroman, I.; Bourbigot, S. *Polym. Degrad. Stabil.* **2010**, *95*, 315.
11. Chen, X. L.; Jiao, C. M. *J. Therm. Anal. Calorim.* **2011**, *104*, 1037.
12. Chrysler Corporation U.5.2.623.866.1952
13. Dynamit Nobel Aktiengesellschaft "Industrio An:eiger" No 65.1527.1963.
14. Hirohata, T.; Misaki, T.; Yoshii, M. *J. Soc. Mater. Sci. Jpn.* **1987**, *36*, 185.
15. Hirohata, T.; Misaki, T.; Komodo, S.; Yoshii, M. *J. Soc. Mater. Sci. Jpn. (Japanese)* **1989**, *38*, 1098.
16. Gao, J. G.; Liu, Y.; Yang, L. *Polym. Degrad. Stabil.* **1999**, *63*, 19.
17. Gao, J. G.; Liu, Y.; Wang, F. *Eur. Polym. J.* **2001**, *37*, 207.
18. Gao, J. G ,Xia, L. Y. *Polym. Degrad. Stabil.* **2004**, *83*, 71.
19. Xia, L. Y.; Gao, J. G.; Yu, Z. X. *Chem. J. Inter.* **2004**, 062013Pe.
20. Liu, Y. F.; Gao, J. G.; Zhang, R. Z. *Polym. Degrad. Stabil.* **2002**, *77*, 495.
21. Zhang, M.; Wei, J. F.; Xie, F.; Jun, J. *Chin. J. Synth. Chem.* **2004**, *12*, 77.
22. Liu, H. C.; Wu, L. J.; You, Y. S.; Feng, D. Y.; Mao, R. Z. *Eng. Plast. Appl.* **2007**, *35*, 51.
23. Drevelle, C.; Lefebvre, J.; Duquesne, S.; Le Bras, M.; Poutch, F.; Vouters, M.; Magniez, C. *Polym. Degrad. Stabil.* **2005**, *88*, 130.